ADVANCED MATERIALS
www.advmat.de

Color Fine-Tuning of CNTs@AAO Composite Thin Films via Isotropically Etching Porous AAO Before CNT Growth and Color Modification by Water Infusion

By *Xianglong Zhao, Guowen Meng,* Qiaoling Xu, Fangming Han,* and *Qing Huang*

Optical interference structures exist in nature, e.g., in feathers of birds and wings of insects, and exhibit vivid colors, which originate from the mechanism of optical interference and thus can vary notably with the viewing-angle and the refractive index of the dielectric medium surrounding the optical interference structures.[1–3] Because of the attractive applications of optical interference structures in color display, decoration, anti-counterfeiting and liquid sensors, considerable attention has been paid to the construction of man-made systems with interference colors, such as multilayer structures,[4] silicon dimple arrays,[5] and anodic aluminum oxide (AAO) thin films embedded with metal.[6,7] Recently, it has been reported that AAO thin films embedded with carbon nanotubes (CNTs) (denoted as CNTs@AAO composite thin films) display brilliant colors, which stem from the interference between the reflected light from the AAO top planar surface and the emergent light reflected on the AAO–Al interface.[8] As colors of the CNTs@AAO composite thin films are mainly determined by the interference band with the maximum reflectance (B_{max}) in the visible region, and B_{max} shifts by changing the AAO film thickness, color tuning of the CNTs@AAO composite thin films can be attained by varying the AAO film thickness in the anodization. However, B_{max} is very sensitive to the thickness of the AAO film, and the pore growth rate of the AAO in the anodization is very fast, so it would be difficult for this approach to tune the color of the CNTs@AAO composite thin film in a well-controlled manner. In addition, the as-prepared CNTs@AAO composite thin films are hydrophobic and thus prohibit water infusion.[9] If the CNTs@AAO composite thin films can be changed into hydrophilic, the composite thin films might be used as water sensors. Here, by applying wet-chemical etching to porous AAO thin films to thin the AAO films and widen the AAO pores isotropically before CNTs growth, controllable precise color tuning of the CNTs@AAO composite thin films has been achieved. Moreover, via further plasma cleaning, the CNTs@AAO composite thin films with large AAO pore diameter can change their colors remarkably after water infusion. Additionally, via applying wet-chemical etching to different areas of one piece of AAO film for rationally different durations, patterned CNTs@AAO composite thin film with each area showing a unique color has been obtained. The details of the fabrication of the AAO, the etching of the AAO, and the growth of the CNTs are given in the Experimental section.

Figure 1a and b are SEM images of the CNTs released from the CNTs@AAO composite thin films. Figure 1a shows free-standing CNTs aggregating into clumps and formed inside the pores of the AAO films without being etched. Figure 1b reveals obvious opening of the CNTs formed in the AAO thin films etched in phosphoric acid solution for 17.5 min. Figure 1c is the TEM image of an individual CNT from Figure 1a with outer diameter, wall thickness and length of ~35, ~4, and ~280 nm, respectively. Figure 1d is the TEM image of the CNTs from Figure 1b. The outer diameter and wall thickness of the CNTs are estimated to be 90 and 6 nm, respectively. Therefore, etching AAO films before CNTs growth can cause remarkable increase of the CNTs outer diameter but negligible thickening of the CNT wall.

Because of the copying effect of the template-synthesized CNTs on the size and morphology of pores of the AAO template,[9–12] the outer diameter and the length of the CNTs obtained in our experiment can be taken as pore diameter and pore depth of the AAO film, respectively (Fig. 1e). In addition, it has been reported that the AAO pore diameter is directly proportional to the etching duration.[13] Hence, using the value of the outer diameter of the CNTs produced in the AAO without being etched (~35 nm) and that produced in the AAO with being etched for 17.5 min (~90 nm), we deduce that the widening rate of the AAO pore diameter is $(90–35)/17.5 = \sim 3\ \mathrm{nm\ min^{-1}}$, revealing that the rate of the phosphoric acid solution etching the AAO film is $\sim 1.5\ \mathrm{nm\ min^{-1}}$, because phosphoric acid etches the AAO pores isotropically (Fig. 1f). Since the outer diameter of the CNTs produced in AAO without being etched is ~35 nm, the initial pore radius (r) of the corresponding AAO films is ~17.5 nm. With the AAO films etched in phosphoric acid solution for a period of time (t), r can be expressed as

$$r = 17.5 + 1.5t \quad (1)$$

As shown in Figure 1f, the film thickness of the AAO film can be taken as the sum of the pore depth and the barrier layer

[*] Prof. G. Meng, Dr. X. Zhao, Dr. Q. Xu, Dr. F. Han
Key Laboratory of Materials Physics
Anhui Key Laboratory of Nanomaterials and Nanostructures
Institute of Solid State Physics, Chinese Academy of Sciences
P. O. Box 1129, Hefei 230031 (PR China)
E-mail: gwmeng@issp.ac.cn
Prof. Q. Huang
Key Laboratory of Ion Beam Bioengineering
Institute of Plasma Physics, Chinese Academy of Sciences
Hefei 230031 (P. R. China)

DOI: 10.1002/adma.200904370

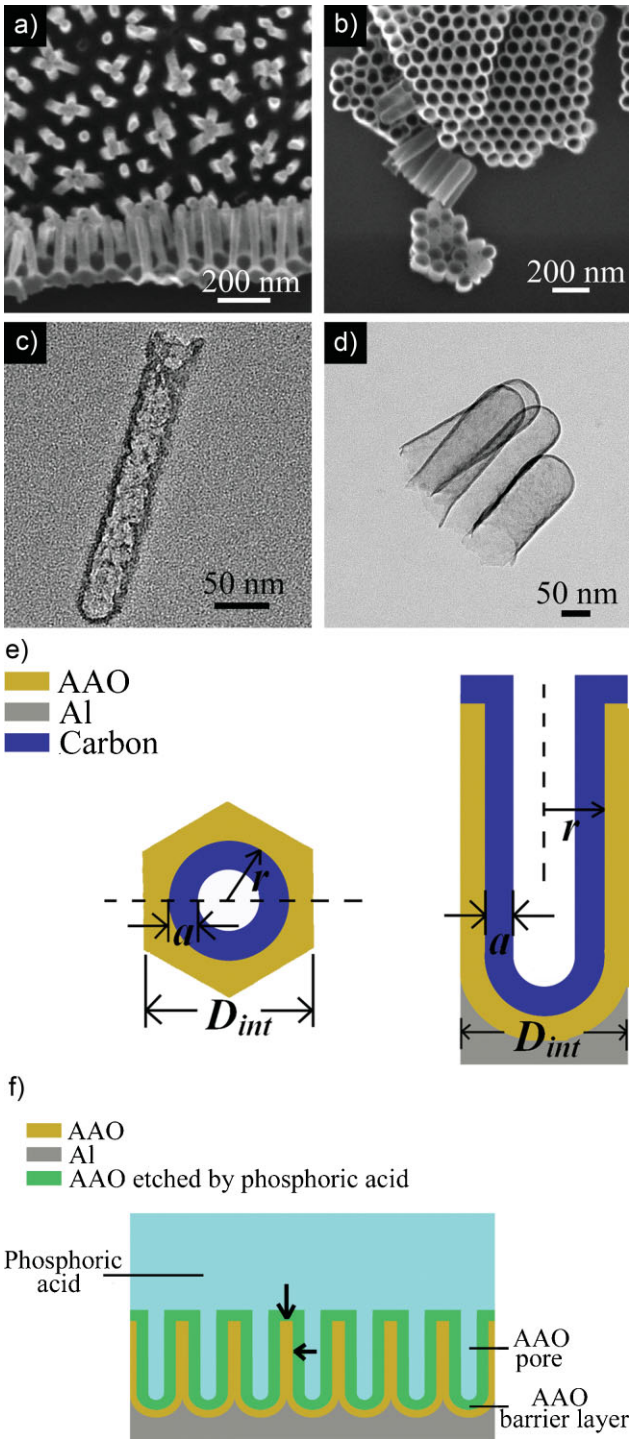

Figure 1. a) and b) SEM images of the CNTs released from AAO (anodizing time: 7 min) without being etched and with being etched for 17.5 min, respectively. c) TEM image of an individual CNT from (a). d) TEM image of the CNTs from b). e) Schematic of the top-view (left) and side-view (right) of one AAO cell embedded with a CNT. Here, r and D_{int} are the pore radius and the inter-pore distance of the AAO, respectively, and a is the wall thickness of the CNT. f) Schematic of the etching process. Phosphoric acid etching can lead to the thinning of the film and the widening of the pore along the direction marked with arrows.

thickness. As just mentioned, the AAO pore depth is the same as the length of the CNT. Therefore, the pore depth of the AAO film without being etched is ~280 nm. It is reported that the AAO barrier layer formed at 40 V is ~50 nm in thickness,[14,15] thus the thickness of the AAO film before being etched is estimated to be 280 + 50 = 330 nm. Since the thinning rate of the AAO film thickness in phosphoric acid solution is the same as the rate of phosphoric acid solution etching the AAO film, the thickness (d) of the AAO film after being etched in phosphoric acid solution for a period of time t can be expressed as

$$d = 330 - 1.5t \quad (2)$$

Figure 2a shows the colors of the CNTs@AAO composite thin films, illustrating that the color gradually changes from salmon pink to cyan with the increase of the etching duration from 0 to 17.5 min with a constant increment of 3.5 min. Figure 2b shows UV–Vis diffuse reflectance spectra of the CNTs@AAO composite thin films. Corresponding to the color evolution from salmon pink to cyan in Figure 2a, the interference band B_{max} of the CNTs@AAO composite thin films shifts from ~632 to 498 nm with the etching duration elongated from 0 to 17.5 min, revealing that the shifting rate of B_{max} with the etching duration is (632–498)/17.5 = ~7.7 nm min^{-1}, which is much smaller than that induced by controlling the anodizing duration (~630 nm min^{-1}) reported previously.[8] Therefore, controlling the duration of etching porous thin AAO films before CNTs growth is a more desirable approach to precise color tuning of the CNTs@AAO composite thin films.

When the constructive interference takes place (Fig. 2c), the wavelength (λ) at the maximum reflectance in each interference band shown in the UV–vis diffuse reflectance spectra can be obtained by

$$\lambda = 2nd\cos\theta/m \quad (3)$$

where θ is the refraction angle, m the interference order, d the film thickness and n is the refractive index of the CNTs@AAO composite thin films.[8] In comparison with the thickness of the CNTs@AAO composite thin film, the thickness of the carbon layer on top of the AAO film is negligible, hence, the thickness of the CNTs@AAO composite thin film can be taken as that of the AAO film, and it also decreases with the increase of the etching duration. Using the values of the AAO film thickness (calculated from Eq. 2) and the well-resolved interference bands (in Fig. 2b), we deduced the wavelength dependence of the refractive index of the composite thin films, which is shown in Figure 2d. It can be seen that in visible light region, the refractive index of each composite thin film slightly increases with the decrease of the wavelength,[8] and with the increase of the etching duration from 0 to 17.5 min, the refractive index of the CNTs@AAO composite thin films decreases from ~1.92 to 1.64. Therefore, according to Equation 3, both the thinning of the film and the decrease of the refractive index should be responsible for the blue-shift of the interference bands of the CNTs@AAO composite thin films.

Since the film thickness of the CNTs@AAO composite thin film is the same as that of the AAO film, the thinning rate of the composite thin film is the same as that of the AAO film

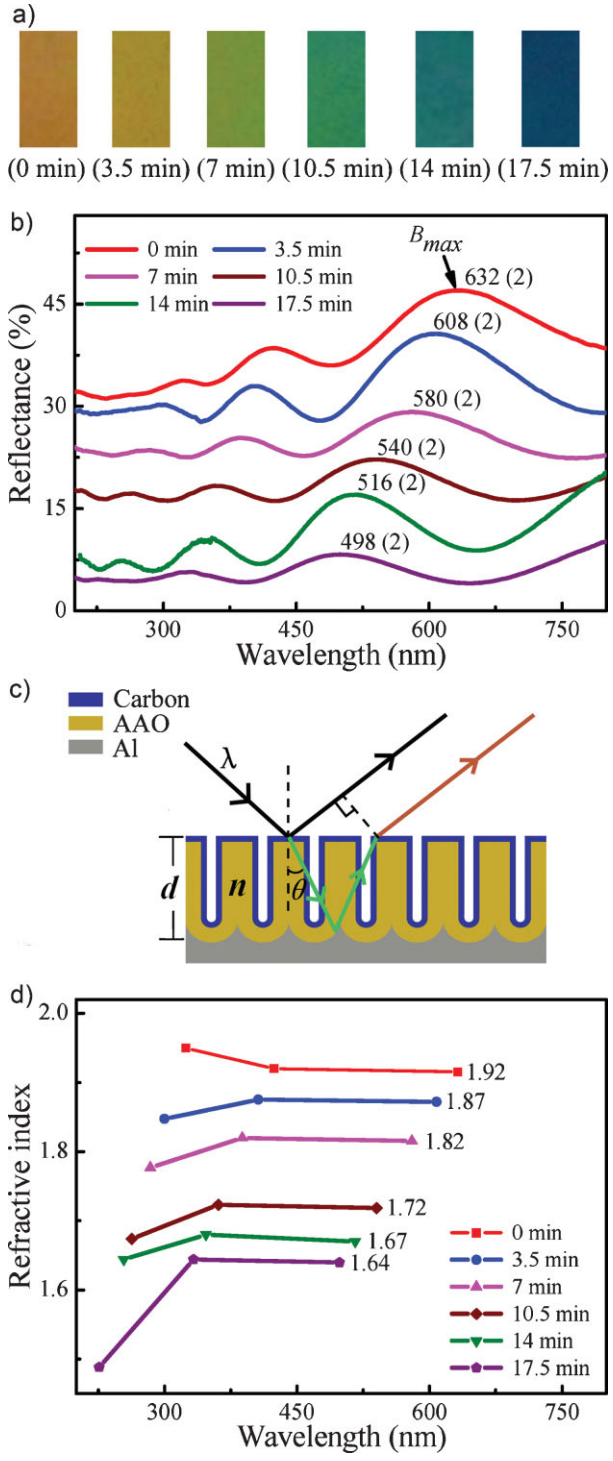

Figure 2. a) Photographs (with viewing angle of ~0°) of the CNTs@AAO composite thin films where the AAO films (anodizing duration: 7 min) were etched for different periods of time (marked below the photograph) from 0 to 17.5 min (with the time increment of 3.5 min) before CNTs growth. b) UV–vis diffuse reflectance spectra of the composite thin films shown in (a). The interference band B_{max} of each composite thin film is marked. The numbers within the brackets correspond to the interference order of B_{max}. c) Schematic of the optical interference of the composite thin film. d) Dependence of the refractive index on wavelength for the composite thin films in a. The mean refractive index in visible light region for each composite thin film is marked.

(~1.5 nm min^{-1}). Using the value of the refractive index of the CNTs@AAO composite thin film with AAO without being etched (~1.92) and that with AAO etched for 17.5 min (~1.64), the decrease rate of the refractive index of the composite thin film with the etching duration is (1.92–1.64)/17.5 = ~0.016 min^{-1}. Hence, compared with the high decrease rate of the film thickness (~160 nm min^{-1}) achieved by governing the anodizing duration,[8] our approach via controlling the duration of etching AAO films makes both the film thickness and the refractive index of the composite thin films decrease at a much lower rate, leading to color fine-tuning of the CNTs@AAO composite thin films.

As shown in Figure 1e, the pore radius of the CNTs@AAO composite thin film is the difference between the AAO pore radius r and the CNT wall thickness (a). Thus, considering the hexagonal feature of the AAO cell, the porosity (P, volume fraction of pores) of the composite thin film can be expressed as

$$P = \frac{2\pi(r-a)^2}{\sqrt{3}D_{int}^2} \quad (4)$$

According to Equations 1 and 4, the porosity of the CNTs@AAO composite thin film increases with the elongation of the etching duration. Because porosity increase can give rise to the reduction of the refractive index for porous material,[16,17] the decrease of the refractive index of the CNTs@AAO composite thin films may thus be ascribed to the porosity increase induced by AAO pore widening.

Plasma cleaning could improve hydrophilic property of the film surface.[18] For this reason, we subjected the CNTs@AAO composite thin films shown in Figure 2a to plasma cleaning and then dripped water on their top surfaces. As a result, we found that when the etching time of the AAO is longer than 7 min (i.e., the AAO pore diameter is larger than ~56 nm, as calculated from Eq. 1), the CNTs@AAO composite thin films could change their colors remarkably, as shown in Figure 3a. Figure 3b shows UV–Vis diffuse reflectance spectra of the CNTs@AAO composite thin films in Figure 3a with water covering their top surfaces. Corresponding to the color variation of the water-covered region of the composite thin films in Figure 3a, the interference band B_{max} decreases from ~634 to 528 nm with the increase of the etching duration from 0 to 17.5 min. Therefore, in comparison with the B_{max} in Figure 2b, water covering can induce the red-shift of B_{max} of the composite thin films. Furthermore, in correspondence with the remarkable color change resulting from dripping water on the top surfaces of the composite thin films, this red-shift is more pronounced when the etching time is longer than 7 min. For example, when the etching duration is 0 and 3.5 min, the red-shift of B_{max} is 2 and 4 nm, respectively. While the etching duration is prolonged to 7, 10.5, 14, and 17.5 min, the red-shift is increased to 18, 24, 32, and 30 nm, respectively.

Using the values of the AAO film thickness (calculated from Eq. 2) and the well-resolved interference bands (in Fig. 3b), we deduced the refractive index of the CNTs@AAO composite thin films, which is shown in Figure 3c. In visible region, the refractive index of the composite thin film, which varies little with wavelength, decreases from ~1.92 to 1.74 with the etching duration increased from 0 to 17.5 min. Hence, compared with the refractive index of the composite thin films without being covered

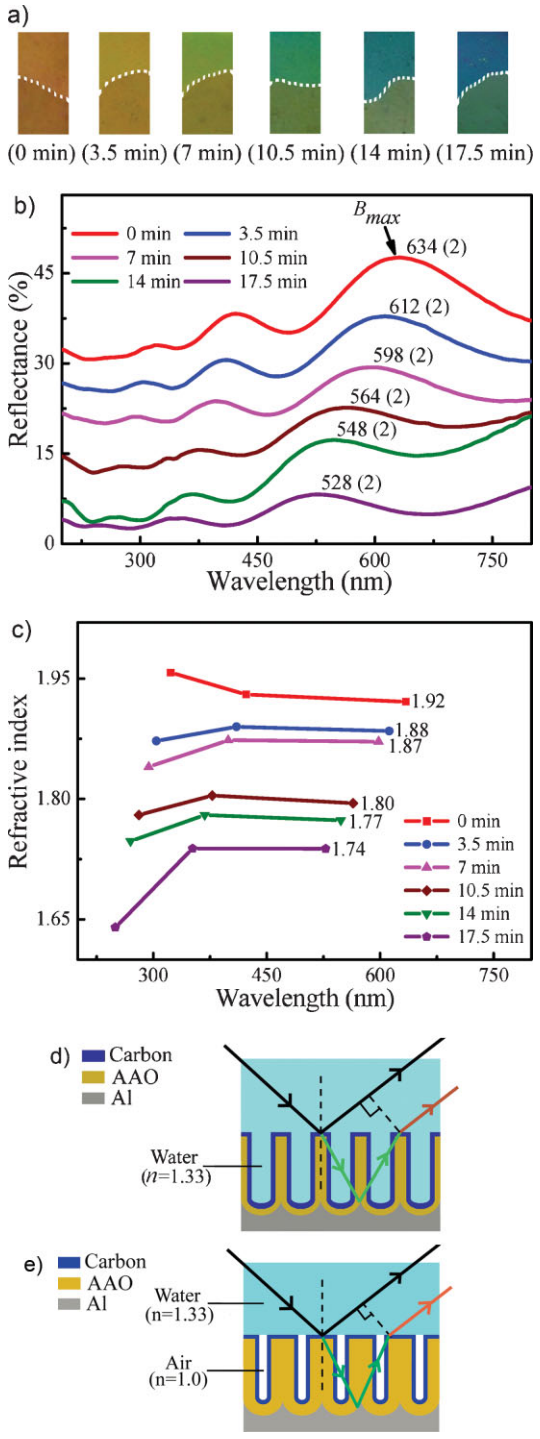

Figure 3. a) Photographs (with viewing angle of ~0°) of the plasma-cleaned CNTs@AAO composite thin films (shown in Fig. 2a) without (above the white dotted line) and with (below the white dotted line) water covering their top surfaces. b) UV–vis diffuse reflectance spectra of the composite thin films in a) with water covering their top surfaces. The interference band B_{max} and its corresponding interference order (within the brackets) for each composite thin film are marked. c) Dependence of the refractive index on wavelength for the composite thin films in a) with water covering their top surfaces. The mean refractive index in visible light region for each composite thin film is marked. d,e) Schematic of the plasma-cleaned composite thin films with and without water infusion, respectively.

by water (shown in Fig. 2d), the water covering can give rise to the increase of the refractive index, which is more obvious when the etching duration is longer than 7 min.

It is well known that the effect of the plasma cleaning originates from the plasma bombardment. Therefore, for CNTs@AAO composite thin films with large pore diameter, their pore interior may be easily modified to hydrophilic owing to the easy entry of the plasma, causing the easy infusion of water into their pores (Fig. 3d). As refractive index of water (~1.33) is larger than that of air (~1.0), the water infusion can hence bring increase of the refractive index of the CNTs@AAO composite thin films with large pores. On the contrary, for CNTs@AAO composite thin films with small pore diameter, because their pore interior can not be modified hydrophilic easily, water may only covers their top surfaces (Fig. 3e). In this case, little increase of the refractive index of the composite thin films can be achieved. Therefore, the remarkable color change of the CNTs@AAO composite thin films with AAO etched for longer than 7 min can be attributed to their refractive index increase induced by water infusion.

It has been reported that one piece of AAO film with different thickness in different areas can be achieved via anodizing different areas of Al foil for different durations, and accordingly patterned CNTs@AAO thin film with different colors in different areas can be obtained after growth of the CNTs in the patterned AAO film.[8] Since both the color's hues and values can be rationally predesigned, the patterned CNTs@AAO composite thin films are of particular interest in both decoration and anti-counterfeiting applications. Here, by applying wet-chemical etching to different areas in one piece of AAO thin film for different durations to achieve differences in both the film thickness and the pore diameter, patterned CNTs@AAO composite thin film was obtained after CNTs growth. For instance, by repeating two consecutive process of covering part of the AAO with adhesive tapes and etching the remaining part for three times before the CNTs growth, we have obtained patterned CNTs@AAO composite thin film (Fig. 4a), where AAO has four areas, with both the film thickness and the pore diameter varying from one area to another. It can be seen that all colors of the patterned composite thin film change obviously with viewing angle (Fig. 4b), and some colors are able to change noticeably after dripping water on the top surface of the patterned composite thin film (Fig. 4c), due to large pores induced by long-time etching of the AAO film. Furthermore, by writing English words (or characters) and Chinese words on the top surfaces of the AAO films with a ball pen before wet-chemical etching (the pores in the written area could not be etched), difference in both the film thickness and the pore diameter between the handwriting area and the rest can make CNTs@AAO composite thin films record the previous person's handwriting, as shown in Figure 4d–f. In this way, writing style of the individuals could be recorded on the CNTs@AAO composite thin films, revealing the function of the patterned composite thin film as personal information recognizer in anti-counterfeiting technology.

In conclusion, by employing phosphoric acid etching to reduce the film thickness and increase the pore diameter of the AAO thin films before CNTs growth, slow decrease of both film thickness and refractive index of the CNTs@AAO composite thin films has been achieved, resulting in precise color tuning of the CNTs@AAO composite thin films. Additionally, water infusion

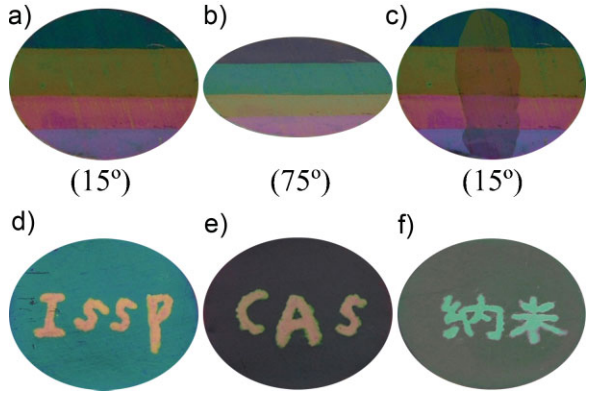

Figure 4. a–c) Photographs of the patterned CNTs@AAO composite thin films with AAO (anodizing duration: 7.5 min) etched for 0, 5, 10 and 15 min (from the bottom to the top), respectively, i.e., the AAO pore diameter of the patterned CNTs@AAO composite thin films in each photograph (from the bottom to the top) is ~35, ~50, ~65 and ~80 nm, respectively. The viewing angle in a, b, and c is ~15°, ~75°, and ~15°, respectively, and water covers part of the top planar surface of the patterned composite thin film in c. d–f) Photographs of the patterned composite thin films (with viewing angle of ~15°) where AAO films were anodized for d) 7 min, e) 11 min, and f) 15 min, respectively. The patterned parts of the AAO ("ISSP," "CAS," and the Chinese words) were not etched (AAO pore diameter: ~35 nm), and the remaining parts were etched for 17 min (AAO pore diameter: ~86 nm).

can remarkably change the colors of the plasma-cleaned CNTs@AAO composite thin films with AAO wet-chemically etched for longer than 7 min, being ascribed to the easy hydrophilization of pore interior of the CNTs@AAO composite thin films. Furthermore, patterned CNTs@AAO composite thin film with different areas showing different colors has been achieved via etching different areas of one piece of AAO film for different durations before CNTs growth. The vivid CNTs@AAO composite thin films may have potentials in dye/pigment-free displays, decoration, liquid sensors, micro-fluidics, and anti-counterfeiting technology.

Experimental

The AAO thin films were fabricated via a two-step anodizing process [10,19]. The first anodization was carried out at a constant voltage of 40 V in 0.3 M oxalic acid at 1 °C for 6 h. The formed alumina film was then chemically removed by immersing it in a mixture of phosphoric acid (6 wt%) and chromic acid (1.8 wt%) at 60 °C for 3 h. Subsequently, the second anodization was conducted for 7 min under the same conditions as those in the first-step. The isotropic etching of the porous AAO was finally carried out by immersing the AAO thin films on the remaining Al in a 10 wt% phosphoric acid aqueous solution at 30 °C. Then the CNTs were grown inside the pores of the etched AAO via chemical vapor deposition at 650 °C for 2 h with 4 sccm of C_2H_2 as precursor and 120 sccm of Ar as carrying gas [12,20].

The CNTs released from the CNTs@AAO composite thin films were characterized by using scanning electron microscopy (SEM, SIRION 200) and transmission electron microscopy (TEM, JEM-2010). Diffuse reflectance spectra of the CNTs@AAO composite thin films were recorded by an UV–vis spectrometer (U-4100), and incident light was projected onto the composite thin film with a near normal configuration. The Ar plasma cleaning was carried out by using a plasma cleaner (PDC-32G, high power) for 20 s.

Acknowledgements

We thank the National Natural Science Foundation of China (Grant No. 50972145, 10975152, and 50525207) and the National Basic Research Program of China (Grant 2007CB936601) for financial support.

Received: December 21, 2009
Revised: January 28, 2010
Published online: May 11, 2010

[1] A. R. Parker, *J. Opt. A: Pure Appl. Opt.* **2000**, *2*, R15.
[2] H. W. Yin, L. Shi, J. Sha, Y. Z. Li, Y. H. Qin, B. Q. Dong, S. Meyer, X. H. Liu, L. Zhao, J. Zi, *Phys. Rev. E* **2006**, *74*, 051916.
[3] S. Kinoshita, S. Yoshioka, J. Miyazaki, *Rep. Prog. Phys.* **2008**, *71*, 076401.
[4] R. W. Phillips, A. F. Bleikolm, *Appl. Opt.* **1996**, *35*, 5529.
[5] H. J. Lezec, J. J. McMahon, O. Nalamasu, P. M. Ajayan, *Nano Lett.* **2007**, *7*, 329.
[6] E. Strazzi, F. Yincenzi, S. Bellei, *Aluminium Finish.* **1997**, *17*, 20.
[7] H. M. Chen, C. F. Hsin, R. S. Liu, S. F. Hu, C. Y. Huang, *J. Electrochem. Soc.* **2007**, *154*, K11.
[8] X. H. Wang, T. Akahane, H. Orikasa, T. Kyotani, Y. Y. Fu, *Appl. Phys. Lett.* **2007**, *91*, 011908.
[9] H. Chun, M. G. Hahm, Y. Homma, R. Meritz, K. Kuramochi, L. Menon, L. Ci, P. M. Ajayan, Y. J. Jung, *ACS Nano* **2009**, *3*, 1274.
[10] J. Li, C. Papadopoulos, J. Xu, *Nature* **1999**, *402*, 253.
[11] T. Yanagishita, M. Sasaki, K. Nishio, H. Masuda, *Adv. Mater.* **2004**, *16*, 429.
[12] G. W. Meng, Y. J. Jung, A. Y. Cao, R. Vajtai, P. M. Ajayan, *Proc. Natl. Acad. Sci. USA* **2005**, *102*, 7074.
[13] J. Choi, G. Sauer, K. Nielsch, R. B. Wehrspohn, U. Gösele, *Chem. Mater.* **2003**, *15*, 776.
[14] M. S. Hunter, P. Fowle, *J. Electrochem. Soc.* **1954**, *101*, 481.
[15] W. Lee, R. Ji, U. Gösele, K. Nielsch, *Nat. Mater.* **2006**, *5*, 741.
[16] W. Theisz, *Surf. Sci. Rep.* **1997**, *29*, 91.
[17] S. Walheim, E. Schäffer, J. Mlynek, U. Steiner, *Science* **1999**, *283*, 520.
[18] A. L. Sumner, E. J. Menke, Y. Dubowski, J. T. Newberg, R. M. Penner, J. C. Hemminger, L. M. Wingen, T. Brauers, B. J. Finlayson-Pitts, *Phys. Chem. Chem. Phys.* **2004**, *6*, 604.
[19] H. Masuda, M. Satoh, *Jpn. J. Appl. Phys.* **1996**, *35*, L126.
[20] Y. C. Sui, B. Z. Cui, L. Martínez, R. Perez, D. J. Sellmyer, *Thin Solid Films* **2002**, *406*, 64.